



Spatial distribution and post-depositional diffusion of stable water isotopes in East Antarctica

Mahalinganathan Kanthanathan¹, Thamban Meloth¹, Tariq Ejaz¹, Bhikaji L Redkar¹, and Laluraj C Madhavanpillai¹

¹National Centre for Polar and Ocean Research, Headland Sada, Vasco-da-Gama, Goa – 403804

Correspondence: K. Mahalinganathan (maha@ncpor.res.in)

Abstract. We have analysed the spatial variations in the mean stable water isotopic values, snow accumulation patterns and moisture sources along coast to inland transects in central Dronning Maud Land (cDML) and Princess Elizabeth Land (PEL) regions of East Antarctica. The δD and $\delta^{18}O$ varied systematically from coastal to inland regions in cDML and PEL regions in response to the surface air temperature. While the elevation effect was not clearly visible, the isotope variations appeared to be associated with snow accumulation in cDML region and temperature in PEL region, which ultimately are associated with elevation. Further, a clear influence of topography on the snow accumulation was observed in cDML region. Such an observation was not recorded in PEL transect, apparently due to the strong snow redistribution in this region due to katabatic winds. The moisture sources to the study areas were identified using HYSPLIT backtrajectory calculations. The major sources of precipitation during summer arrived from the south Atlantic ocean in the cDML and the Indian Ocean in PEL. During winter, the sources of precipitation in cDML extended upto Weddell Sea while in PEL, the sources extended upto 50°S in the Indian Ocean. In order to understand the post-depositional isotope diffusion processes in firn, a firn core which was drilled close to the cDML transect, five years after the snow core transect, was analysed in comparison with snow records. Our study showed a significant isotope amplitude diffusion with a diffusion length of 6 cm from the surface to 4 m depth in 5 years.

1 Introduction

Ever since Dansgaard (1964) successfully explained the dependency of stable isotopic composition of precipitation on physical parameters such as temperature, latitude and altitude, the stable water isotopes (δD and $\delta^{18}O$) have become the primary proxy tool in paleoclimate studies. As a result, the high resolution δD and $\delta^{18}O$ records from the polar regions have been continuously used to interpret the temperature and snow accumulation information from decadal to millennial time scales (e.g. EPICA, 2006; 2k PMIP3 group, 2015). However, the stable water isotope records in Antarctic snow depends on multiple factors such as the temperature of the moisture source region where evaporation occur, followed by fractionation due to subsequent condensation and evaporation cycles during transport and finally the temperature at which the precipitation forms (Landais et al., 2017).



Though ice core δD and $\delta^{18}O$ records are often assumed to represent climatic signals of an entire region, spatial variation of these isotope records indicate complex signals that are often not straightforward to interpret. Factors such as accumulation rates, erosion and redistribution by wind contributes to such variations in spatial scale (Fisher et al., 1985; Town et al., 2008). Another important factor that could influence the isotope based climate records in Antarctic ice is the role of extreme precipitation events (Turner et al., 2019). The deuterium excess (d), which is a second-order parameter defined by combination of δD and $\delta^{18}O$ ($d = \delta D - 8 \cdot \delta^{18}O$), reflects the behaviour of these two isotopic species occurring during the kinetic and equilibrium fractionation (Jouzel and Merlivat, 1984). The association between ‘ d ’ and the climatic parameters such as the surface temperature, relative humidity and the wind speed in the moisture source region have been established in previous studies (Jouzel et al., 1982; Jouzel and Merlivat, 1984; Petit et al., 1991).

Paleoclimate studies based on ice cores primarily rely on stable water isotope records to provide paleoclimate information. However, these stable isotope records are modified post deposition by diffusion processes (Johnsen, 1977; Whillans and Grootes, 1985). Even though the stable isotope composition in top layers of snow and firn is influenced by diffusion of water vapour and snow densification (Cuffey and Steig, 1998; Hörhold et al., 2011), no net change in isotopic composition were observed due to these processes. The diffusion rate in ice beneath the firn is negligible and therefore gets preserved for much longer time after surviving the diffusion in the top layers (Johnsen, 1977). Studies by Steen-Larsen et al. (2014) and Ritter et al. (2016) have shown isotopic exchanges in the boundary layer on daily scale and on diurnal scales in the polar regions. The isotope signals on the near-surface snow and firn undergo fractionation due to sublimation and condensation processes as observed both in-situ and laboratory studies (Stichler et al., 2001; Sokratov and Golubev, 2009). Apart from the temperature-based fractionation, other factors such as relative humidity and wind speed also influence the post-depositional variations in the ice core isotope signals.

The climate records in ice cores reflect the conditions at which snowfall occurred. These records are influenced by various parameters such as the season at which the precipitation occur and variations in sources of moisture for precipitation. In order to better interpret the ice core stable isotope records, it is important to understand their present variability and interrelationships using modern precipitation and surface snow. The present study analyses the spatial variability of stable water isotopes in terms of latitudinal and altitudinal effects, variation in snow accumulation rates and possible moisture sources in two geographically distinct regions of East Antarctica – Princess Elizabeth Land (PEL) and central Dronning Maud Land (cDML). We also discuss the effect of diffusion of stable isotope signals in the top layers of snow by comparing with the data from an ice core that was drilled close to the transect in the cDML region.

2 Materials and Methods

The study regions are in two different sectors of East Antarctica – the Princess Elizabeth Land (PEL) and the central Dronning Maud Land (cDML), facing the Indian Ocean and the Atlantic Ocean sectors, respectively (Fig. 1). Majority of snow cores (41) were recovered from PEL and cDML transects during the same austral summer of 2008–09 and five more cores were recovered from the inland section of cDML during 2009–10. The transects were categorized into coastal, mountainous and inland regions



based on topography as mentioned in detail in our earlier publications (Mahalinganathan et al., 2012; Mahalinganathan and Thamban, 2016). The snow cores were collected using KOVACS Mark IV system and each core was typically 1 meter long and 14 cm diameter. After recovery, the snow cores were transferred directly into pre-cleaned high-density polyethylene bags and sealed immediately to avoid contamination during storage and shipped under frozen conditions to the National Centre for Polar and Ocean Research, India. The cores were stored at -20°C till analysis. The snow cores were sub-sampled at a 5 cm resolution under a clean laminar hood. A total of 667 sub-samples were processed where the outer layers were removed manually by a clean ceramic knife and the innermost cube was utilized for density measurements from which the snow accumulation rate values were calculated (Mahalinganathan et al., 2012). A portion of each sub-sample was transferred to a 10 mL teflon vials and sealed for further stable isotope analyses.

All sub-samples were melted and immediately analysed for δD and $\delta^{18}\text{O}$ values in the Ice Core Laboratory of National Centre for Polar and Ocean Research using a dual inlet, Isoprime Isotope Ratio Mass Spectrometer, following standard procedures (Naik et al., 2010) which had an external precision of 0.05‰ . Fresh samples were also analysed using a unique laser-based Off-Axis – Integrated Cavity Output Spectroscopy (OA-ICOS) Triple Isotope Water Analyser (TIWA) by Los Gatos Research. The melted samples were introduced directly into the TIWA using a Hamilton $1.2\ \mu\text{L}$ zero dead volume syringe via an auto injector equipped with a heated (85°C) injector block. In order to eliminate inter sample memory effect, four preparatory injections (injections which are not measured), followed by five measurement injections were run for each sample. The last five injections were averaged to produce a single, high-throughput sample measurement. The analytical precision of measurements for δD was $\pm 0.5\text{‰}$ and $\delta^{18}\text{O}$ was $\pm 0.1\text{‰}$ using the TIWA system. Details of sampling locations and analytical results are provided in tables 1 and 2 for cDML and PEL, respectively.

The seasonality in snow cores was determined by establishing the summer and winter peaks in isotope records where a minimum amplitude of 4‰ between summer and winter was used to differentiate these peaks as detailed in figure 2 our previous publications (Mahalinganathan et al., 2012; Mahalinganathan and Thamban, 2016). Near-surface temperature measurements were estimated for the year 2008 from Regional Atmospheric Climate Model version 2.3 (RACMO 2.3) output with a horizontal resolution of 27 km (Wessem et al., 2014). Isotope results from an ice core (IND33/B8, $\sim 101\ \text{m}$) drilled close to the cDML transect was used in order to estimate the diffusion of stable water isotopes in firn. The firn diffusion model originally described in Johnsen et al. (2000) was employed to estimate the diffusion length using the equations provided in Gkinis et al. (2014), Dee et al. (2015) and Münch and Laepple (2018). These calculations were performed using the measurements from the ice core site (site specific parameters) with an average firn density of $340\ \text{kg m}^{-3}$, a mean surface temperature of -22°C , local mean surface pressure of 800 mbar and a local accumulation rate of $300\ \text{kg m}^{-2}\text{yr}^{-1}$. The density and local accumulation rates were directly measured from the snow cores and ice core data while the temperature and local mean surface pressure values were derived from the RACMO output.



3 Results

Snow accumulation rates at both cDML and PEL regions were generally high (averaged values) and reduced from coastal to inland sections as expected (Tables 1 and 2). Accumulation in the coastal section of cDML ranged between 313–410 kg m⁻²yr⁻¹ (mean 354 kg m⁻²yr⁻¹) while in the inland section, it ranged between 104–250 kg m⁻²yr⁻¹ (mean 154 kg m⁻²yr⁻¹) with the mountainous section ranging between 200–320 kg m⁻²yr⁻¹ (mean 235 kg m⁻²yr⁻¹). In PEL, the snow accumulation ranged between 156–390 kg m⁻²yr⁻¹ (mean 276 kg m⁻²yr⁻¹) in the coastal section, while in the inland section it ranged between 138–376 kg m⁻²yr⁻¹ (mean 261 kg m⁻²yr⁻¹).

Stable isotope values and related parameters for snow core sites from both cDML and PEL transects are provided in Tables 1 and 2. All snow cores from both transects showed clear seasonal variations in stable isotope values except for the cores at 240 km in cDML transect and 70 and 100 km in PEL transect, where seasonality could not be established, presumably due to core damage during transportation.

The relationship between δD and $\delta^{18}O$ from all snow cores were assessed using linear regression analysis (Fig. 2). The analysis showed a strong correlation between δD and $\delta^{18}O$ in both cDML (orange circles) and PEL (green circles) transects from coastal to inland region. The slope of the PEL transect (8.12) was close to that of the global meteoric water line (Craig, 1961) with the equation $\delta D = 8.12 \times \delta^{18}O + 7.10$ while the cDML transect followed the linear equation $\delta D = 7.9 \times \delta^{18}O + 2.66$. The relationship between average $\delta^{18}O$ values and annual mean temperature (RACMO 2.3 values) at each snow core site in both transects showed linearity with equations $\delta^{18}O = 0.70 \times T - 14.75$ in cDML region and $\delta^{18}O = 1.01 \times T - 5.70$ in PEL (Fig. 3).

Deuterium excess (d) was calculated for each 5 cm sub-sample of all the snow cores. The d values varied between -1.97‰ and 17.18‰ in cDML and -3.43‰ and 11.10‰ in PEL region. The relationship between near-surface temperature and 'd' was analysed using linear regression method which showed a significant relationship for samples from cDML region with the regression equation: $d = -0.11 \times T + 2.78$. ($R = -0.41$, $p < 0.01$). For the PEL region however, no significant relationship was found (Fig. 4).

Results from the isotope firn diffusion calculations using the R package by Münch and Laepple (2018) revealed a diffusion length of 6 cm over a period of 5 years (Fig. 5).

Five-day back-trajectory frequency maps of coastal, mountainous and inland locations showed vast differences in the sources between summer and winter (Fig. 6). During winter, the air parcels to cDML coast arrived from Weddell Sea and south Atlantic ocean while during summer the trajectories were mostly arriving from the Indian Ocean. Similarly, the air parcels to cDML inland arrived from the Weddell Sea, south Atlantic and the Indian Ocean. The air mass to PEL arrived predominantly from south Indian Ocean during summer and winter.



4 Discussion

4.1 Spatial variability of snow accumulation and stable water isotopes

Spatial variations of snow accumulation in Antarctica are primarily due to the presence of physical barriers during snowfall and snow redistribution post deposition (Melvold et al., 1998; Vaughan et al., 1999). The accumulation rates in cDML region showed a large spatial variation with the near-coastal section having a substantially high average accumulation of $354 \text{ kg m}^{-2} \text{ yr}^{-1}$ (Table 1). Compared to this, the interior section of the transect had less than half of the accumulation rate than the coast (average $155 \text{ kg m}^{-2} \text{ yr}^{-1}$), while the mountainous section showed moderately high accumulation rate (average $235 \text{ kg m}^{-2} \text{ yr}^{-1}$). Such large spatial variability in cDML region can be attributed to the presence of extensive mountain chains existing parallel to the coast. These mountain chains in cDML act as a physical barrier to the air masses arriving from the Southern Ocean impacting the snow accumulation and redistribution. As a result, the study area could be separated into three distinct accumulation regimes. The physiography and topography of the cDML region evidently influenced the snow accumulation rates showing a strong correlation with distance and elevation (Table 3). On the contrary, the PEL transect showed moderately high accumulation with little variation between the coastal ($276 \text{ kg m}^{-2} \text{ yr}^{-1}$) and the inland ($260 \text{ kg m}^{-2} \text{ yr}^{-1}$) sections. Although there exist substantial slope ($> 8 \text{ m km}^{-1}$) in the coast of PEL (Mahalinganathan et al., 2012), it did not affect the overall accumulation rates in the region. Such uniform accumulation pattern in PEL transect could be explained by snowdrift and redistribution induced by strong katabatic winds in this region (Allison, 1998; Ding et al., 2020). With no orographic barriers to influence the flow of katabatic winds, the accumulation pattern in PEL tend to get smoothed by the wind scouring and snow redistribution.

The mean values of $\delta^{18}\text{O}$ and δD from each core location decreased from coastal to inland in both cDML and PEL regions suggesting the typical continental effect, i.e. depletion of $\delta^{18}\text{O}$ and δD with the increasing distance and elevation from the moisture source (Tables 1 and 2). However, the multiple regression models using the geographical parameters and $\delta^{18}\text{O}$ showed negligible variance with distance and elevation (Table 4). Based on these regressions in cDML region, the snow accumulation changes were found to be the primary driver for spatial variations in $\delta^{18}\text{O}$ and δD values. Surface temperature also had noticeable effect on isotopic values in this region (Table 4). However, in the PEL region, the snow accumulation did not play any role in the spatial variations of $\delta^{18}\text{O}$ and δD while temperature played a crucial role. The distance from coast and elevation are known to impact the isotopic composition variation in Antarctic snow (e.g. Huybrechts et al., 2000; Masson-Delmotte et al., 2008). However, there are large regional variations and within short transects, such relationships may not be linear. Since accumulation and temperature parameters are directly impacted by the distance from the coast and elevation, they have indirect influence on the isotopic change.

The relationship between $\delta^{18}\text{O}$ and δD was determined using all the snow cores and the local meteoric water lines (LMWL) for this region were calculated (Fig. 2). The $\delta^{18}\text{O}$ values in cDML region (orange circles) were more depleted than that of the PEL region (green circles). Though the coastal sections in cDML and PEL appears to be almost on the same latitude ($\sim 69^\circ\text{S}$), a difference of 6 ‰ was observed between the coasts. This could be due to the fact that the sampling in cDML begin from 110 km inland while the sampling in PEL begins 10 km from the open ocean. The slope of the LMWL in cDML (7.9) is lower



than that of the global meteoric water line (GMWL) while the slope of LMWL in PEL (8.12) had a slope close to GMWL. The cDML transect, therefore, have a slope closer to that of the Antarctic meteoric water line (AMWL), while the PEL transect have a slope closer to that of the GMWL. All the samples were utilized to observe the $\delta^{18}\text{O}$ and δD relationship which did not appear to show any deviation from the AMWL.

155 The $\delta^{18}\text{O}$ –temperature relationship vary depending on the location of the sampling sites. An Antarctic wide study by Masson-Delmotte et al. (2008) obtained a slope of 0.80‰ per degree Celsius, where the spatial slopes were calculated considering a radius of 400 km, thereby smoothing out the regional topography and moisture source areas. The annual $\delta^{18}\text{O}$ –Temperature relationship is known to be weak in the coastal zones around Antarctica (Goursaud et al., 2019; Bertler et al., 2011; Thomas et al., 2013). Isaksson and Karlén (1994) observed a poor correlation between $\delta^{18}\text{O}$ and Temperature below
160 1000 m a.s.l and a significant correlation above 1000 m a.s.l. The present study includes all such topographic variations as it covers a small region from coast and inland. In spite of such complications, the results from the present study area (Fig. 3) showed that with an increase of every $\delta^{18}\text{O}$ ‰ value, there was an increase in the temperature by 0.7°C in cDML and 1°C in PEL. Therefore, the proposed spatial slope (0.80‰/°C) by Masson-Delmotte et al. (2008) seems to be reasonable.

The deuterium excess (d) values did not show any correlation with any geographical parameters in both cDML and PEL
165 transects (Table 3). An Antarctic-wide compilation of datasets by Masson-Delmotte et al. (2008) showed that even though both elevation and distance appear to generally control d, results from locations below 2000 m elevations did not produce any satisfactory correlation. The PEL transect in this study had only two sampling sites above 2000 m elevation, while the d above 2000 m altitude in cDML transect did not show any meaningful correlation with the geographic parameters. This could be due to involvement of other factors such as regional differences in moisture sources (Simmonds et al 2003). A significant
170 negative correlation was observed between surface temperature and d in cDML (Fig. 4). This negative correlation could be associated with various factors such as the changes in moisture sources, kinetic fractionation on ice crystals at supersaturation point (Jouzel and Merlivat, 1984) and increase of d along the distillation path (Masson-Delmotte et al., 2008).

4.2 Extent and impact of isotope diffusion

Stable water isotope records undergo rapid diffusion in snow and firn than in solid ice (Johnsen, 1977; Whillans and Grootes,
175 1985). As a result, the seasonal amplitude of these records is homogenized in firn – resulting in a considerable reduction in the summer and winter δ values. Since these records are the primary tool in understanding the relationship between isotope ratios and temperature, it is important to estimate the amount of isotope diffusion.

In order to understand the extent of such diffusion in a high accumulation region like the cDML transect, we compared the isotope records of a snow core (cDML 9) with that of a shallow ice core close to the snow transect, IND–33/B8 (Fig. 1). This
180 ice core was drilled 5 years after the snow cores were retrieved (2013–14 Summer). The detailed stable isotope records and chronology of this ice core is discussed in an upcoming paper (Tariq et al., 2020, unpublished). A direct comparison of $\delta^{18}\text{O}$ values of the ice core to a snow core from the transect showed a considerable amount of diffusion in the seasonal amplitude of $\delta^{18}\text{O}$ (Fig. 5). The snow cores originally had an amplitude >5‰ while the ice core seasonal amplitude was reduced to 2‰.



Further, to analyse the extent and impact of isotope diffusion in this core site, the diffusion length was estimated using a firn
185 diffusion model (Johnsen et al., 2000), using the site specific temperature (-22°C), surface firn density (340 kg m^{-3}), local
mean surface pressure (800 mbar) and the local accumulation rate ($300\text{ kg m}^{-2}\text{yr}^{-1}$). The degree of smoothing of the stable
water isotope record depends on the isotopic diffusion length which is shown to increase in the topmost firn layer (Johnsen
et al., 2000). Differential diffusion (σ) was calculated using the equation $\sigma = \sqrt{\sigma^2(z_2) - \sigma^2(z_1)}$, where z_1 and z_2 are initial and
final depths (Münch et al., 2016; Münch and Laepple, 2018). Results from firn diffusion model on the 33/B8 ice core showed
190 a diffusion length of around 6 cm in the surface to a depth of 4 m (Fig. 5, inset). The calculation showed a rapid increase in
diffusion length from the surface before attaining a maximum at 30 meters. This findings can be used during interpretation of
stable isotope record of deep ice cores by removing the effects of diffusion on inter-annual variability.

4.3 Sources of moisture for precipitation in the region

The sources of moisture in Antarctica is widely distributed and strongly influenced by topography, sea-ice conditions and mid-
195 latitude land-ocean contrasts (Sodemann and Stohl, 2009). Moisture source regions could be identified using several techniques.
For instance, d was used as a tracer in isotope models by Petit et al. (1991) and Ciais and Jouzel (1994). An attempt was made
to understand the moisture origin by tracing backwards in time, the air parcels from different sampling sites.

Five-day air parcel backward trajectory frequency map showed moisture source regions close to 60°S latitude during summer
and up to 50°S latitude during winter (Fig. 6). The cDML region had moisture sources from the Weddell sea and south Atlantic
200 Ocean during winters while during summer, the sources were much restricted to the southern Atlantic and Indian Ocean. This
observation is also in line with the results from the cDML region (Rahaman et al., 2016). The winter (JJA) trajectories had
a much wider spread in comparison to summer (DJF) due to the storminess in the southern hemisphere in winter. Also, the
expanding sea ice conditions during the winter blocks the local moisture source contributions to these regions (Sodemann
and Stohl, 2009). About 90% of the trajectories converged along the coastal patch covering predominantly ice shelves, ice
205 rises and the ice cap itself with a small amount covering the sea-ice and open ocean region, strictly followed the orography
of this region with the southern bounds up to various mountain ranges (Queen Fabiola, Sir Rondane, Wohlthat mountains)
along 72°S . In summer, this converging zone with 90% trajectories extended up to 42°E (Prince Olav coast). As a result of
more widespread trajectory distribution in winter, this zone shifted slightly westward extending between 35°E and 8°E . About
50% of the trajectories from coastal section of cDML transect had a wider distribution covering 15°W – 70°E and 60° – 75°S
210 while a small number of trajectories ($\sim 10\%$) originated beyond 55°S from the Southern Ocean and 75°S in the continent. In
winter, the trajectories had a much wider coverage extending between 30°W – 70°E and 57° – 80°S . Similarly, trajectories from
the coastal and inland regions of PEL showed a predominant distribution towards east of the transect with 90% of trajectories
converging up to 100°E (Shackleton ice shelf) in summer and up to 110°E in winter. The southern bounds of the trajectories
were controlled by steep orography – with 2000 m elevation limit. In summer, about 50% of the trajectories in coastal section of
215 PEL extended between 60° – 75°S and 50° – 140°E with an increase of about 5° spread in winter. The inland section of transect
had moisture sources all the way between 60° – 80°S . In summary, the moisture sources in both cDML and PEL regions were
strongly controlled by orography, with highly mixed sources originating from the Southern Ocean.



5 Conclusions

Our study explored the spatial variations in snow accumulation, stable isotopic variations, the moisture sources as well as the post-depositional isotope diffusion in coastal Antarctica. The snow accumulation in central Dronning Maud Land (cDML) region was affected by the mountainous topography while in the Princess Elizabeth Land (PEL) region accumulation pattern smoothed due to the absence of orographic influence. The stable water isotopes from high resolution snow cores sampled from the same season from different regions in Antarctica aided in understanding the spatial variations and to investigate the influences of meteorological and geographical controls. The $\delta^{18}\text{O}$ -T relationship showed a relationship of $0.7\text{‰ }^{\circ}\text{C}^{-1}$ in cDML and $1\text{‰ }^{\circ}\text{C}^{-1}$ in PEL. Considering the spatial variations in $\delta^{18}\text{O}$ -T gradients and the complex difference between snow and firn samples within the continent, careful consideration should be exercised during the application of paleoclimate reconstruction. Comparison of snow core isotope data with the firn core revealed a considerable diffusion with time, showing a diffusion length of about 6 cm from the surface to the depth of 4 m in 5 years. Moisture source studies in this region showed that the majority of the air masses to cDML originated from the south Atlantic (up to 50°S) and Weddell sea during winter and mainly south Atlantic in summer. Within the PEL region, the source was mainly from the Indian Ocean sector.

Author contributions. All authors contributed equally to the work presented in this paper. K. Mahalinganathan collected snow cores and the ice core, analysed data and wrote the paper. Tariq Ejaz and Redkar B.L. analysed the samples. Laluraj C.M. analysed data and contributed to the development of this manuscript. M. Thamban collected the ice core, analysed data and wrote the paper.

Competing interests. The authors declare that the research was conducted in the absence of any commercial or financial relationships that could be construed as a potential conflict of interest.

Acknowledgements. We thank the director of the National Centre for Polar and Ocean Research for his encouragement. Ministry of Earth Sciences is thanked for financial support under the project "Cryosphere and Climate". We are grateful for the support from the members and logistic crew of the 28th and 33rd Indian Scientific Expedition to Antarctica. We thank Dr. Thomas Münch for the R packages to estimate firn diffusion length. We also thank the Norwegian Polar Institute for the Quantarctica QGIS package. This is NCAOR contribution number xx/xxxx.



References

- 2k PMIP3 group, P.: Continental-scale temperature variability in PMIP3 simulations and PAGES 2k regional temperature reconstructions over the past millennium, *Climate of the Past*, 11, 1673–1699, <https://doi.org/10.5194/cp-11-1673-2015>, <https://www.clim-past.net/11/1673/2015/>, 2015.
- 245 Allison, I.: Surface climate of the interior of the Lambert Glacier basin, Antarctica, from automatic weather station data, *Annals of Glaciology*, 27, 515–520, 1998.
- Bertler, N., Mayewski, P., and Carter, L.: Cold conditions in Antarctica during the Little Ice Age—Implications for abrupt climate change mechanisms, *Earth and Planetary Science Letters*, 308, 41–51, 2011.
- Ciais, P. and Jouzel, J.: Deuterium and oxygen 18 in precipitation: Isotopic model, including mixed cloud processes, *Journal of Geophysical Research: Atmospheres*, 99, 16 793–16 803, <https://doi.org/10.1029/94JD00412>, <https://agupubs.onlinelibrary.wiley.com/doi/abs/10.1029/94JD00412>, 1994.
- 250 Craig, H.: Isotopic Variations in Meteoric Waters, *Science*, 133, 1702–1703, <https://doi.org/10.1126/science.133.3465.1702>, <http://science.sciencemag.org/content/133/3465/1702>, 1961.
- Cuffey, K. M. and Steig, E. J.: Isotopic diffusion in polar firn: implications for interpretation of seasonal climate parameters in ice-core records, with emphasis on central Greenland, *Journal of Glaciology*, 44, 273–284, <https://doi.org/10.3189/S0022143000002616>, 1998.
- 255 Dansgaard, W.: Stable isotopes in precipitation, *Tellus*, 16, 436–468, <https://doi.org/10.1111/j.2153-3490.1964.tb00181.x>, <https://onlinelibrary.wiley.com/doi/abs/10.1111/j.2153-3490.1964.tb00181.x>, 1964.
- Dee, S., Emile-Geay, J., Evans, M. N., Allam, A., Steig, E. J., and Thompson, D.: PRYSM: An open-source framework for PRoXY System Modeling, with applications to oxygen-isotope systems, *Journal of Advances in Modeling Earth Systems*, 7, 1220–1247, <https://doi.org/10.1002/2015MS000447>, <https://agupubs.onlinelibrary.wiley.com/doi/abs/10.1002/2015MS000447>, 2015.
- 260 Ding, M., Yang, D., van den Broeke, M. R., Allison, I., Xiao, C., Qin, D., and Huai, B.: The Surface Energy Balance at Panda 1 Station, Princess Elizabeth Land: A Typical Katabatic Wind Region in East Antarctica, *Journal of Geophysical Research: Atmospheres*, 125, e2019JD030 378, <https://doi.org/10.1029/2019JD030378>, <https://agupubs.onlinelibrary.wiley.com/doi/abs/10.1029/2019JD030378>, e2019JD030378 2019JD030378, 2020.
- 265 EPICA, C. M.: One-to-one coupling of glacial climate variability in Greenland and Antarctica., *Nature*, 444, 195, 2006.
- Fisher, D. A., Reeh, N., and Clausen, H.: Stratigraphic noise in time series derived from ice cores, *Annals of Glaciology*, 7, 76–83, 1985.
- Gkinis, V., Simonsen, S., Buchardt, S., White, J., and Vinther, B.: Water isotope diffusion rates from the NorthGRIP ice core for the last 16,000 years – Glaciological and paleoclimatic implications, *Earth and Planetary Science Letters*, 405, 132 – 141, <https://doi.org/10.1016/j.epsl.2014.08.022>, <http://www.sciencedirect.com/science/article/pii/S0012821X14005287>, 2014.
- 270 Goursaud, S., Masson-Delmotte, V., Favier, V., Preunkert, S., Legrand, M., Minster, B., and Werner, M.: Challenges associated with the climatic interpretation of water stable isotope records from a highly resolved firn core from Adélie Land, coastal Antarctica, *The Cryosphere*, 13, 1297–1324, <https://doi.org/10.5194/tc-13-1297-2019>, <https://www.the-cryosphere.net/13/1297/2019/>, 2019.
- Hörhold, M. W., Kipfstuhl, S., Wilhelms, F., Freitag, J., and Frenzel, A.: The densification of layered polar firn, *Journal of Geophysical Research: Earth Surface*, 116, <https://doi.org/10.1029/2009JF001630>, <https://agupubs.onlinelibrary.wiley.com/doi/abs/10.1029/2009JF001630>, 2011.
- 275 Huybrechts, P., Steinhage, D., Wilhelms, F., and Bamber, J.: Balance velocities and measured properties of the Antarctic ice sheet from a new compilation of gridded data for modelling, *Annals of Glaciology*, 30, 52–60, <https://doi.org/10.3189/172756400781820778>, 2000.



- Isaksson, E. and Karlén, W.: Spatial and temporal patterns in snow accumulation, western Dronning Maud Land, Antarctica, *Journal of Glaciology*, 40, 399–409, 1994.
- 280 Johnsen, S.: Stable isotope homogenization of polar firn and ice, *Isotopes and impurities in snow and ice*, 118, 210–219, 1977.
- Johnsen, S. J., Clausen, H. B., Cuffey, K. M., Hoffmann, G., and Creyts, T. T.: Diffusion of stable isotopes in polar firn and ice: the isotope effect in firn diffusion, in: *Physics of Ice Core Records*, edited by Hondoh, T., pp. 121–140, Hokkaido University Press, Sapporo, Japan, 2000.
- Jouzel, J. and Merlivat, L.: Deuterium and oxygen 18 in precipitation: Modeling of the isotopic effects during snow formation, *Journal of Geophysical Research: Atmospheres*, 89, 11 749–11 757, <https://doi.org/10.1029/JD089iD07p11749>, <https://agupubs.onlinelibrary.wiley.com/doi/abs/10.1029/JD089iD07p11749>, 1984.
- 285 Jouzel, J., Merlivat, L., and Lorius, C.: Deuterium excess in an East Antarctic ice core suggests higher relative humidity at the oceanic surface during the last glacial maximum, *Nature*, 299, 688, 1982.
- Landais, A., Casado, M., Prié, F., Magand, O., Arnaud, L., Ekaykin, A., Petit, J.-R., Picard, G., Fily, M., Minster, B., Touzeau, A., Goursaud, S., Masson-Delmotte, V., Jouzel, J., and Orsi, A.: Surface studies of water isotopes in Antarctica for quantitative interpretation of deep ice core data, *Comptes Rendus Geoscience*, 349, 139 – 150, <https://doi.org/https://doi.org/10.1016/j.crte.2017.05.003>, <http://www.sciencedirect.com/science/article/pii/S1631071317300494>, 2017.
- 290 Mahalinganathan, K. and Thamban, M.: Potential genesis and implications of calcium nitrate in Antarctic snow, *The Cryosphere*, 10, 825–836, 2016.
- 295 Mahalinganathan, K., Thamban, M., Laluraj, C. M., and Redkar, B. L.: Relation between surface topography and sea-salt snow chemistry from Princess Elizabeth Land, East Antarctica, *The Cryosphere*, 6, 505–515, 2012.
- Masson-Delmotte, V., Hou, S., Ekaykin, A., Jouzel, J., Aristarain, A., Bernardo, R., Bromwich, D., Cattani, O., Delmotte, M., Falourd, S., et al.: A review of Antarctic surface snow isotopic composition: Observations, atmospheric circulation, and isotopic modeling, *Journal of climate*, 21, 3359–3387, 2008.
- 300 Melvold, K., Hagen, J. O., Pinglot, J. F., and Gunestrup, N.: Large spatial variation in accumulation rate in Jutulstraumen ice stream, Dronning Maud Land, Antarctica, *Annals of Glaciology*, 27, 231–238, <https://doi.org/10.3189/1998AoG27-1-231-238>, 1998.
- Münch, T. and Laepple, T.: What climate signal is contained in decadal-to centennial-scale isotope variations from Antarctic ice cores?, *Climate of the Past*, 14, 2053–2070, 2018.
- 305 Münch, T., Kipfstuhl, S., Freitag, J., Meyer, H., and Laepple, T.: Regional climate signal vs. local noise: a two-dimensional view of water isotopes in Antarctic firn at Kohnen Station, Dronning Maud Land, *Climate of the Past*, 12, 1565–1581, <https://doi.org/10.5194/cp-12-1565-2016>, <https://www.clim-past.net/12/1565/2016/>, 2016.
- Naik, S. S., Thamban, M., Rajakumar, A., D’Souza, W., Laluraj, C., and Chaturvedi, A.: Influence of climatic teleconnections on the temporal isotopic variability as recorded in a firn core from the coastal Dronning Maud Land, East Antarctica, *Journal of earth system science*, 119, 41–49, 2010.
- 310 Petit, J. R., White, J. W. C., Young, N. W., Jouzel, J., and Korotkevich, Y. S.: Deuterium excess in recent Antarctic snow, *Journal of Geophysical Research: Atmospheres*, 96, 5113–5122, <https://doi.org/10.1029/90JD02232>, <https://agupubs.onlinelibrary.wiley.com/doi/abs/10.1029/90JD02232>, 1991.



- Rahaman, W., Thamban, M., and Laluraj, C.: Twentieth-century sea ice variability in the Weddell Sea and its effect on moisture transport: Evidence from a coastal East Antarctic ice core record, *The Holocene*, 26, 338–349, <https://doi.org/10.1177/0959683615609749>, <https://doi.org/10.1177/0959683615609749>, 2016.
- Ritter, F., Steen-Larsen, H. C., Werner, M., Masson-Delmotte, V., Orsi, A., Behrens, M., Birnbaum, G., Freitag, J., Risi, C., and Kipfstuhl, S.: Isotopic exchange on the diurnal scale between near-surface snow and lower atmospheric water vapor at Kohlen station, East Antarctica, *The Cryosphere*, 10, 1647–1663, <https://doi.org/10.5194/tc-10-1647-2016>, <https://www.the-cryosphere.net/10/1647/2016/>, 2016.
- Sodemann, H. and Stohl, A.: Asymmetries in the moisture origin of Antarctic precipitation, *Geophysical Research Letters*, 36, <https://doi.org/10.1029/2009GL040242>, <https://agupubs.onlinelibrary.wiley.com/doi/abs/10.1029/2009GL040242>, 2009.
- Sokratov, S. A. and Golubev, V. N.: Snow isotopic content change by sublimation, *Journal of Glaciology*, 55, 823–828, 2009.
- Steen-Larsen, H. C., Masson-Delmotte, V., Hirabayashi, M., Winkler, R., Satow, K., Prié, F., Bayou, N., Brun, E., Cuffey, K. M., Dahl-Jensen, D., Dumont, M., Guillevic, M., Kipfstuhl, S., Landais, A., Popp, T., Risi, C., Steffen, K., Stenni, B., and Sveinbjörnsdóttir, A. E.: What controls the isotopic composition of Greenland surface snow?, *Climate of the Past*, 10, 377–392, <https://doi.org/10.5194/cp-10-377-2014>, <https://www.clim-past.net/10/377/2014/>, 2014.
- Stichler, W., Schotterer, U., Fröhlich, K., Ginot, P., Kull, C., Gäggeler, H., and Pouyaud, B.: Influence of sublimation on stable isotope records recovered from high-altitude glaciers in the tropical Andes, *Journal of Geophysical Research: Atmospheres*, 106, 22 613–22 620, 2001.
- Thomas, E. R., Bracegirdle, T. J., Turner, J., and Wolff, E. W.: A 308 year record of climate variability in West Antarctica, *Geophysical Research Letters*, 40, 5492–5496, 2013.
- Town, M. S., Warren, S. G., Walden, V. P., and Waddington, E. D.: Effect of atmospheric water vapor on modification of stable isotopes in near-surface snow on ice sheets, *Journal of Geophysical Research: Atmospheres*, 113, <https://doi.org/10.1029/2008JD009852>, <https://agupubs.onlinelibrary.wiley.com/doi/abs/10.1029/2008JD009852>, 2008.
- Turner, J., Phillips, T., Thamban, M., Rahaman, W., Marshall, G. J., Wille, J. D., Favier, V., Winton, V. H. L., Thomas, E., Wang, Z., van den Broeke, M., Hosking, J. S., and Lachlan-Cope, T.: The Dominant Role of Extreme Precipitation Events in Antarctic Snowfall Variability, *Geophysical Research Letters*, 46, 3502–3511, <https://doi.org/10.1029/2018GL081517>, <https://agupubs.onlinelibrary.wiley.com/doi/abs/10.1029/2018GL081517>, 2019.
- Vaughan, D. G., Bamber, J. L., Giovinetto, M., Russell, J., and Cooper, A. P. R.: Reassessment of Net Surface Mass Balance in Antarctica, *Journal of Climate*, 12, 933–946, [https://doi.org/10.1175/1520-0442\(1999\)012<0933:RONSMB>2.0.CO;2](https://doi.org/10.1175/1520-0442(1999)012<0933:RONSMB>2.0.CO;2), 1999.
- Wessem, V. J., Reijmer, C., Lenaerts, J., Berg, V. W., Broeke, V. M., and Meijgaard, V. E.: Updated cloud physics in a regional atmospheric climate model improves the modelled surface energy balance of Antarctica, *The Cryosphere*, 8, 125–135, <https://doi.org/10.5194/tc-8-125-2014>, 2014.
- Whillans, I. and Grootes, P.: Isotopic diffusion in cold snow and firn, *Journal of Geophysical Research: Atmospheres*, 90, 3910–3918, 1985.



Figures

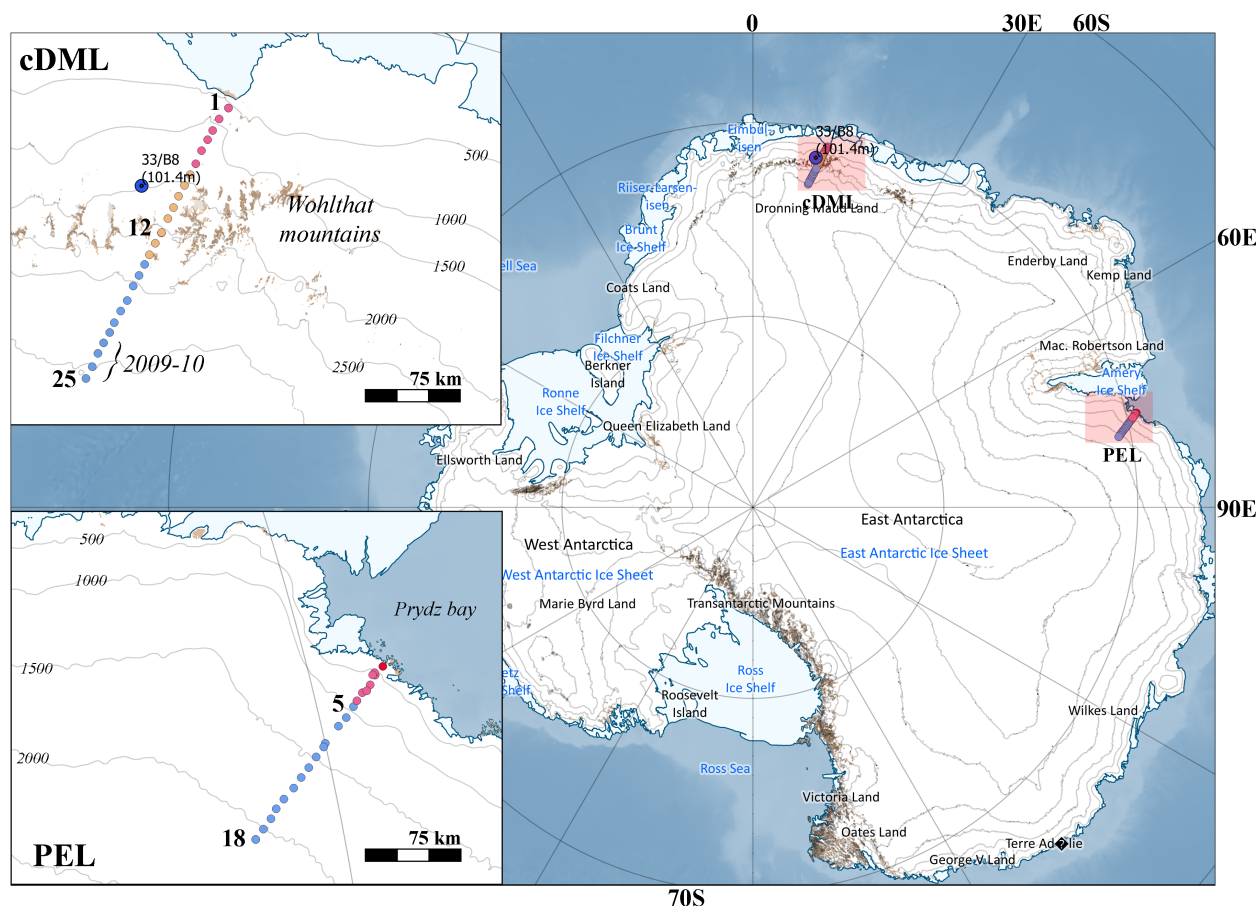


Figure 1. Study region showing sampling locations along the central Dronning Maud Land (cDML) and Princess Elizabeth Land (PEL) in East Antarctica. Colour coded sampling locations indicate coastal (red), mountainous (orange) and inland (blue) regions of the transect. The ice core 33/B8 shown in the cDML region was drilled during 2013–14 field season. Background map sourced from Hillshades and Elevation model compiled using ETOPO1, IBSCO and RAMP2 data.

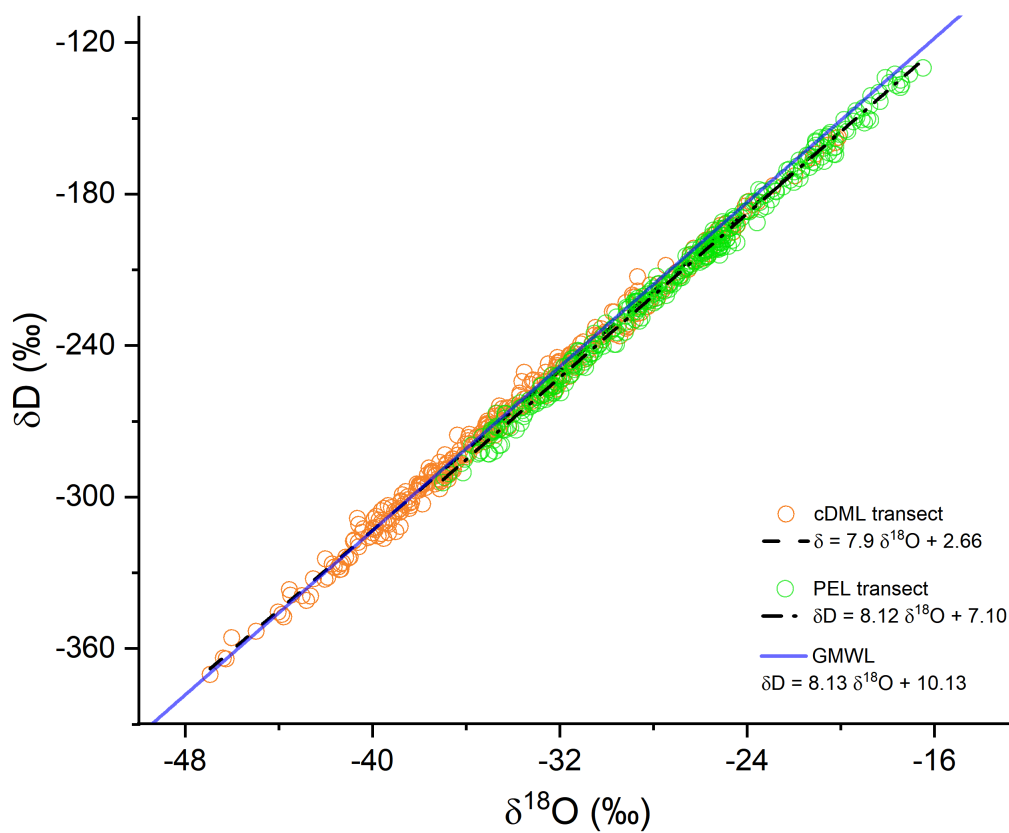


Figure 2. Relationship between δD and $\delta^{18}\text{O}$ in cDML and PEL transects. Blue line is Global Meteoric Water Line.

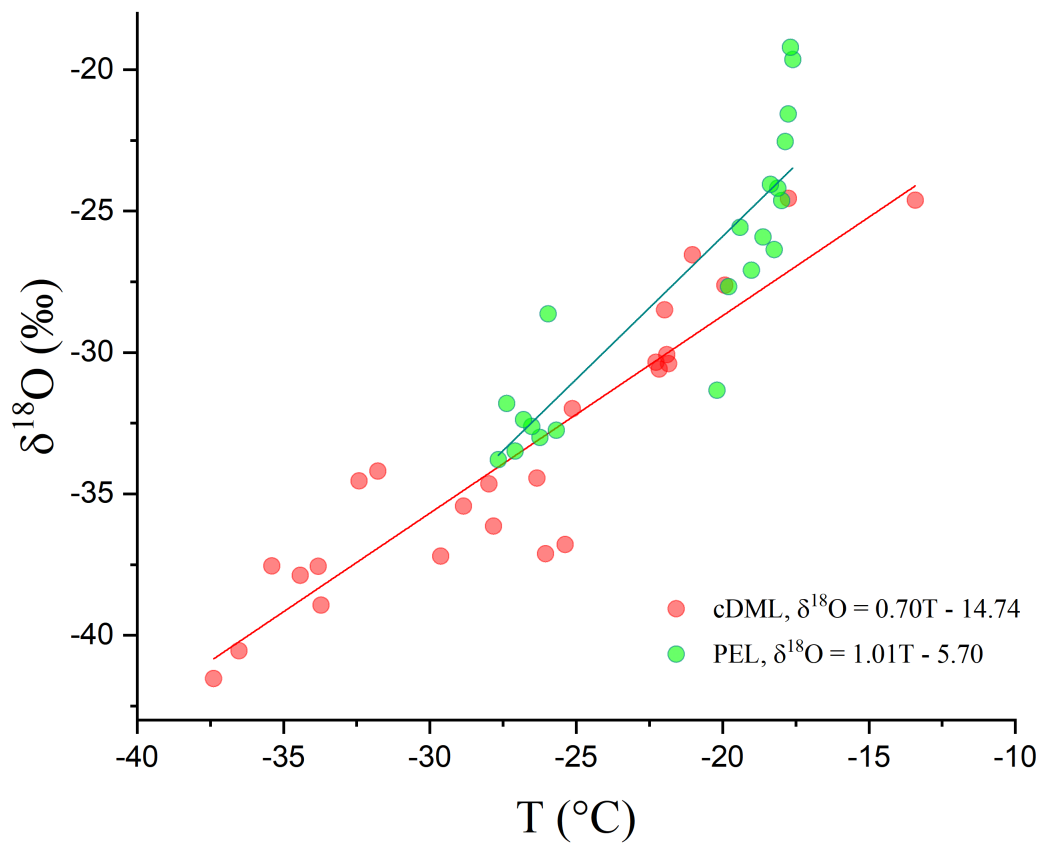


Figure 3. Relationship between mean annual $\delta^{18}\text{O}$ values and annual mean temperature in cDML and PEL transects.

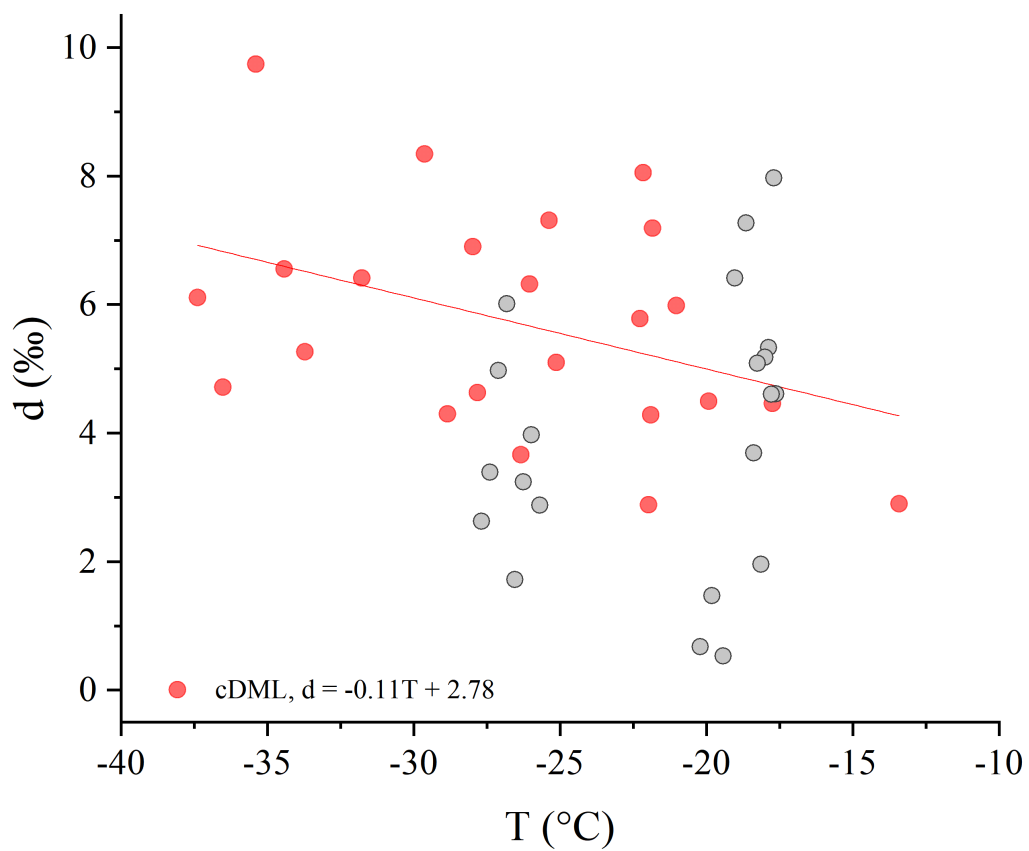


Figure 4. Relationship between deuterium excess and Temperature from cDML and PEL regions.

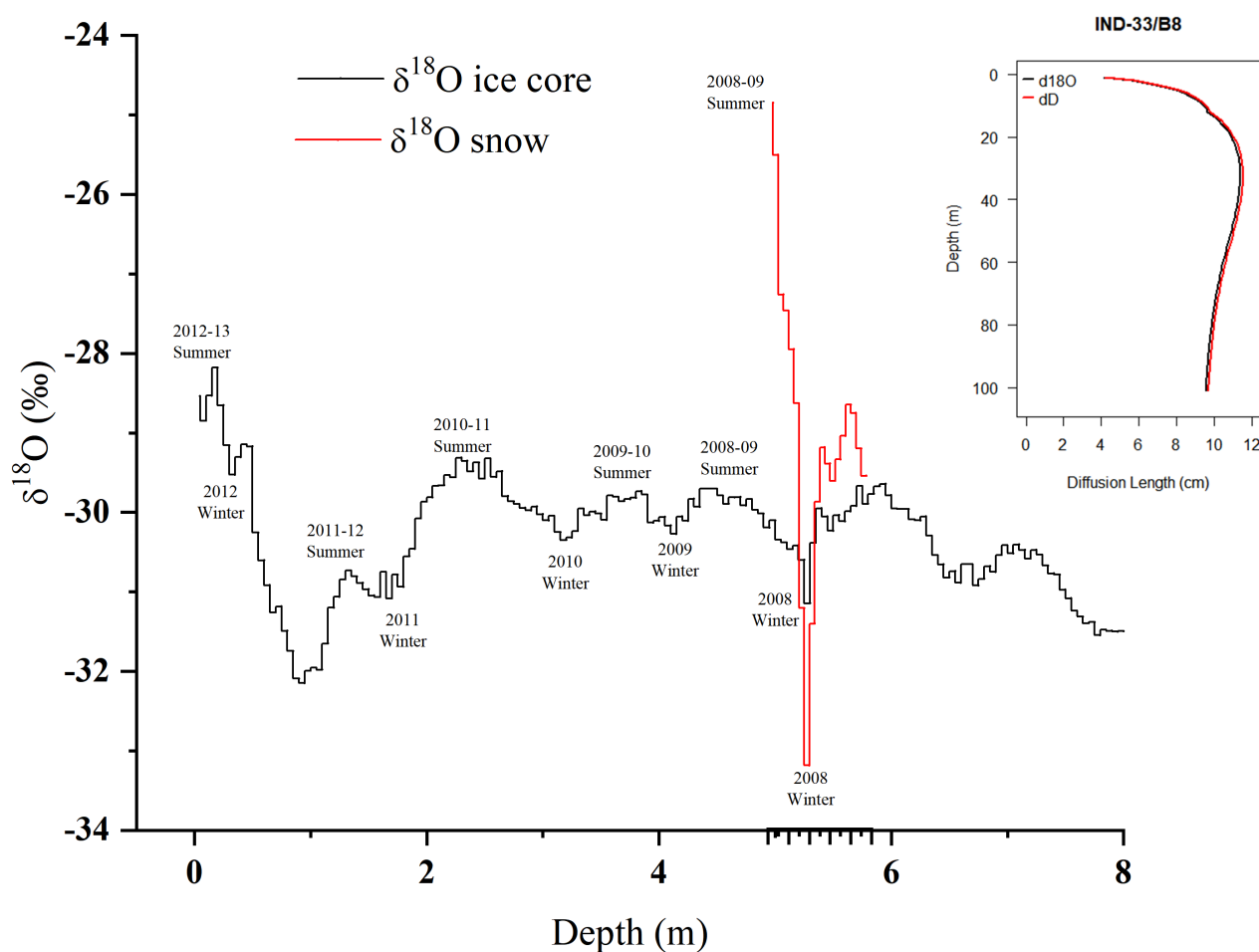


Figure 5. Differences in seasonal amplitude of $\delta^{18}\text{O}$ in snow core and ice core. The ice core was drilled after 5 seasons in 2013–14 summer. The firm diffusion model (inset) calculated based on site specific temperature, pressure and density of surface firm showed a diffusion length of around 6 cm in the surface explaining the amplitude diffusion in ice core.

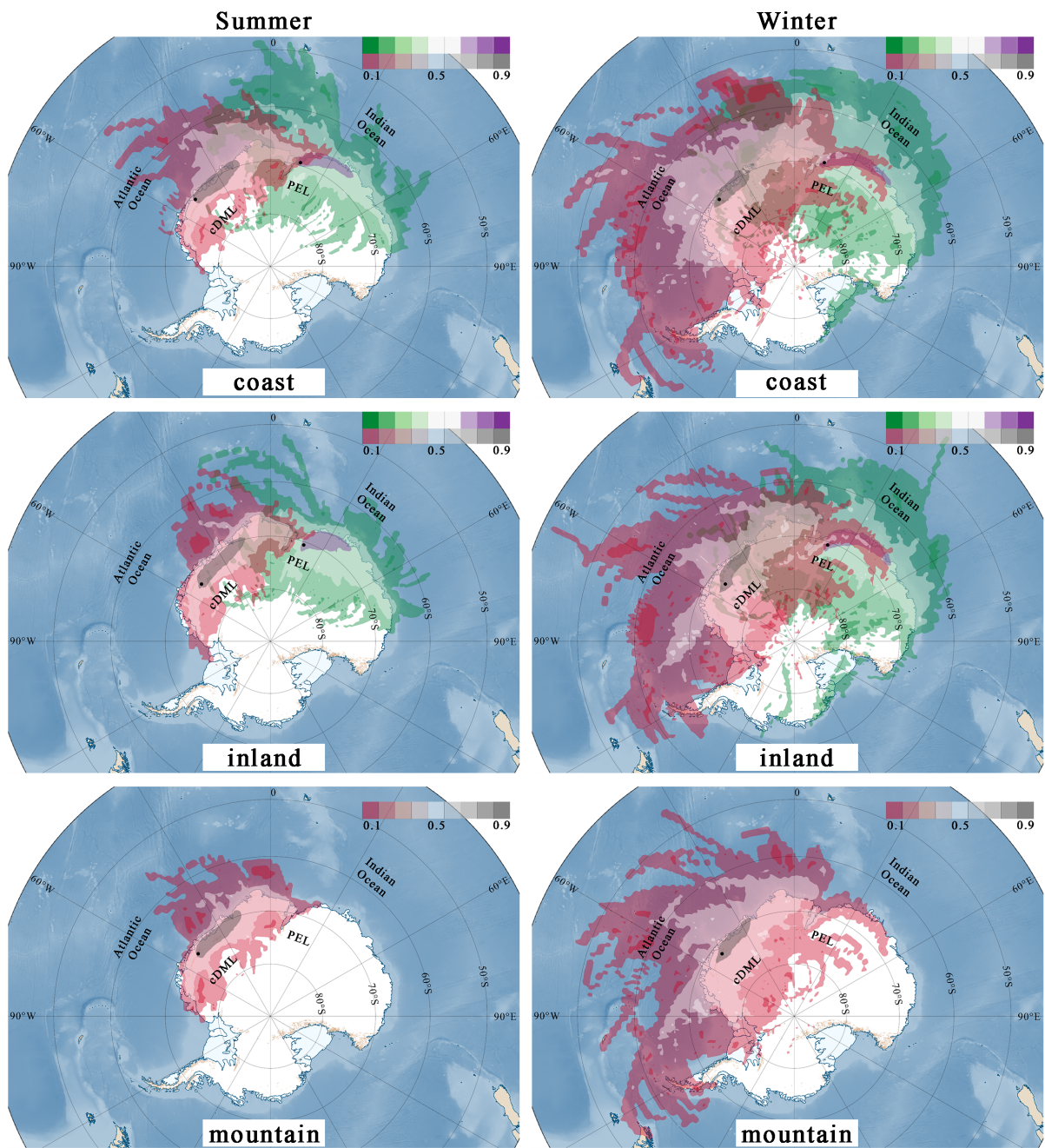


Figure 6. Five-day back-trajectory frequencies in coastal (top), inland (middle) and mountainous sections (bottom panels) of the cDML and PEL transects during the austral summer (left panel) and winter (right). The translucent purple color shows the lowest frequency and the translucent green shows the highest frequency of trajectories arriving to the sampling sites. The frequencies were derived using HYSPLIT model with inputs from meteorological parameters of GDAS dataset. Background map sourced from Hillshades and Elevation model compiled using ETOPO1, IBSCO and RAMP2 data.



345 Tables

Table 1. Geographical distribution and averaged stable isotope values of the snow cores from cDML region.

cDML	Lat S	Lon E	Dis km	Ele m	δD ‰	$\delta^{18}O$ ‰	d ‰	Temp °C	Acc kg m ⁻² yr ⁻¹
1	-70.85	11.74	110	610	-193.97	-24.61	2.90	-13.4	-
2	-70.94	11.59	120	914	-191.90	-24.55	4.46	-17.8	361
3	-71.03	11.53	130	1067	-216.44	-27.62	4.5	-19.9	352
4	-71.12	11.45	140	1158	-206.37	-26.54	5.99	-21	313
5	-71.21	11.37	150	1250	-235.92	-30.39	7.19	-21.8	334
6	-71.3	11.3	160	1341	-236.31	-30.07	4.28	-21.9	410
7	-71.38	11.21	170	1524	-236.57	-30.58	8.05	-22.2	320
8	-71.46	11.14	180	1600	-225	-28.49	2.88	-22	227
9	-71.54	11.06	190	1768	-236.95	-30.34	5.78	-22.3	157
10	-71.64	10.99	200	1890	-250.79	-31.99	5.1	-25.1	226
11	-71.73	10.91	210	2012	-271.83	-34.44	3.66	-26.3	224
12	-71.81	10.83	220	2103	-287.01	-36.79	7.31	-25.4	202
13	-71.89	10.75	230	2225	-290.59	-37.11	6.32	-26	292
14	-71.98	10.67	240	2377	-270.23	-34.64	6.9	-28	-
15	-72.07	10.6	250	2576	-284.43	-36.13	4.63	-27.8	106
16	-72.16	10.51	260	2652	-279.1	-35.43	4.3	-28.8	180
17	-72.23	10.43	270	2743	-289.24	-37.2	8.35	-29.6	207
18	-72.33	10.34	280	2865	-267.1	-34.19	6.41	-31.8	222
19	-72.41	10.25	290	2896	-	-	-	-32.4	249
20	-72.5	10.16	300	3018	-	-	-	-33.8	157
21	-72.57	10.07	310	3045	-306.2	-38.93	5.27	-33.7	126
22	-72.65	9.97	320	3068	-296.47	-37.88	6.55	-34.4	123
23	-72.73	9.88	330	3082	-290.59	-37.54	9.74	-35.4	117
24	-72.83	9.8	340	3101	-319.65	-40.55	4.71	-36.5	110
25	-72.92	9.7	350	3130	-326.09	-41.53	6.11	-37.4	104



Table 2. Geographical distribution and averaged stable isotope values of the snow cores from PEL region.

PEL	Lat S	Lon E	Dis km	Ele m	δD ‰	$\delta^{18}O$ ‰	d ‰	Temp °C	Acc $kg\ m^{-2}\ yr^{-1}$
2	-69.55	76.3	20	300	-152.55	-19.64	4.61	-14.2	227
19	-69.55	76.25	23	579	-145.71	-19.21	7.97	-14.4	156
20	-69.56	76.28	26	640	-167.94	-21.57	4.6	-14.6	269
3	-69.6	76.46	30	792	-175.02	-22.54	5.33	-16.1	389
21	-69.63	76.56	35	884	-191.87	-24.63	5.18	-16.9	200
4	-69.67	76.58	40	975	-191.58	-24.19	1.95	-17.2	329
22	-69.71	76.71	45	1036	-205.81	-26.36	5.08	-17.8	292
5	-69.75	76.81	50	1113	-188.78	-24.06	3.69	-18.5	347
6	-69.81	77	60	1234	-200.06	-25.92	7.27	-19.3	270
7	-69.88	77.13	70	1280	-210.32	-27.09	6.41	-19.8	
8	-70	77.41	87	1494	-204.08	-25.58	0.53	-21.1	376
9	-70.01	77.48	90	1509	-219.93	-27.67	1.47	-21.3	335
10	-70.08	77.65	100	1585	-250.04	-31.34	0.67	-21.8	
11	-70.15	77.83	110	1631	-259.17	-32.76	2.87	-22.3	256
12	-70.21	78	120	1722	-225.12	-28.64	3.97	-22.8	138
13	-70.28	78.18	130	1768	-260.84	-33.01	3.23	-23.2	249
14	-70.36	78.36	140	1875	-259.26	-32.62	1.71	-24	179
15	-70.43	78.53	150	1920	-253.01	-32.38	6.01	-24.5	335
16	-70.48	78.71	160	1987	-262.96	-33.49	4.97	-25	225
17	-70.55	78.9	170	2118	-251.04	-31.8	3.39	-25.8	246
18	-70.61	79.08	180	2210	-267.71	-33.79	2.62	-26.6	263



Table 3. Correlation between stable water isotopes and physical and climate parameters in cDML and PEL regions. All correlations are significant at 0.01 level.

	Distance	Elevation	δD	$\delta^{18}O$	d	Temp	Acc
central Dronning Maud Land							
Distance	1	0.986	-0.936	-0.937	-	-0.985	-0.834
Elevation	0.973	1	-0.937	-0.939	-	-0.974	-0.834
δD	-0.925	-0.946	1	0.999	-	0.923	0.781
$\delta^{18}O$	-0.927	-0.946	0.999	1	-	0.926	0.778
d	-	-	-	-	1	-	-
Temp	-0.983	-0.995	0.948	0.947	-	1	0.794
Acc.	-	-	-	-	-	-	1
Princess Elizabeth Land							

Table 4. Multiple regression model summaries explaining the percentage of stable isotope variability attributed to accumulation, temperature and the physical parameters. Temperature effect is clear in PEL while precipitation effect is dominant in cDML region.

PEL Model		$\delta^{18}O$	
		R	Variance (%)
1	Accumulation	0.109	1.2
2	Accumulation, Temperature	0.952	89.4
3	Acc., Temp., Distance	0.952	0.1
4	Acc., Temp., Distance, Elevation	0.953	0
cDML Model			
1	Accumulation	0.778	60.5
2	Accumulation, Temperature	0.915	23.2
3	Accumulation, Temperature, Distance	0.930	2.9
4	Acc., Temp., Distance, Elevation	0.934	0.7